Journal of Sound and Vibration 329 (2010) 566–584

Contents lists available at ScienceDirect

Journal of Sound and Vibration

journal homepage: www.elsevier.com/locate/jsvi

Damage monitoring in sandwich beams by modal parameter shifts: A comparative study of burst random and sine dwell vibration testing

Amir Shahdin *, Joseph Morlier, Yves Gourinat

Université de Toulouse, ISAE/DMSM, Campus Supaero, 10 av. Edouard Belin BP54032, 31055 Toulouse, France

ARTICLE INFO

Article history:
Received 24 February 2009
Received in revised form
21 September 2009
Accepted 22 September 2009
Handling Editor: H. Ouyang
Available online 24 October 2009

ABSTRACT

This paper presents an experimental study on the effects of multi-site damage on the vibration response of honeycomb sandwich beams, damaged by two different ways i.e., impact damage and core-only damage simulating damage due to bird or stone impact or due to mishandling during assembly and maintenance. The variation of the modal parameters with different levels of impact energy and density of damage is studied. Vibration tests have been carried out with both burst random and sine dwell testing in order to evaluate the damping estimation efficiency of these methods in the presence of damage. Sine dwell testing is done in both up and down frequency directions in order to detect structural non-linearities. Results show that damping ratio is a more sensitive parameter for damage detection than the natural frequency. Design of experiments (DOE) highlighted density of damage as the factor having a more significant effect on the modal parameters and also proved that sine dwell testing is more suitable for damping estimation in the presence of damage as compared to burst random testing.

1. Introduction

Laminated honeycomb sandwich materials are being used widely in weight sensitive structures where high flexural rigidity is required, such as in the aerospace industry. By inserting a light weight core between the two face sheets, the bending stiffness and strength are substantially increased compared with a single layer homogeneous structure, without adding much weight. When the beam or plate undergoes flexural vibration, the damped core is constrained primarily to shear. This shearing causes energy to be dissipated and the flexural motion to be damped. However damage in these structures may negate many of the benefits of sandwich construction. Impact can induce various types of damage in the structure. The facesheets can be damaged through delamination and fiber breakage; the facesheet and core interface region can be debonded and the core can be damaged through crushing and shear failure mechanisms. Safe and functional effectiveness of stressed sandwich structures can often depend on the retention of integrity of each of the different materials used in its manufacture. Therefore lightweight sandwich materials used in next generation of more advanced aircraft, marine craft, road and rail vehicles must possess the capability to absorb higher impact energy and retain a high degree of structural integrity. For aeronautical structures, a field where this problem has been quite studied, the components have to undergo low energy impacts caused by dropped tools, mishandling during assembly and maintenance, and in-service impacts by foreign objects such as stones or birds. In these low energy impacts normally, a small indentation

* Corresponding author. Tel.: +33 5 61 33 83 86; fax: +33 5 61 33 83 30.
E-mail address: amir.shahdin@isae.fr (A. Shahdin).

0022-460X/$ - see front matter © 2009 Elsevier Ltd. All rights reserved.
doi:10.1016/j.jsv.2009.09.029

Nomenclature

BR	burst random testing
C	structural damping matrix (force/velocity)
D1	damaged state at 2 points
D2	damaged state at 4 points
f_k	resonance frequency (Hz) for the kth mode
FRF	frequency response function
$H(\omega)$	frequency response function matrix
j	imaginary axis in the complex plane
K	stiffness matrix (force/displacement)
M	mass matrix
$p(k)$	pole location for the kth mode
$R(k)$	residue magnitude (FRF/s)
SD	sine-dwell testing
UD	undamaged state
ζ_k	damping ratio (percent) for the kth mode
$\sigma(k)$	modal damping for kth mode
$\omega(k)$	modal damped frequency for kth mode (rad/s)
ω_d	damped natural frequency (rad/s)
ω_n	undamped natural frequency (rad/s)
*	complex conjugate

is seen on the impact surface. This level of damage is often referred to as barely visible impact damage (BVID). There has been considerable research on the impact performance and damage development in carbon fiber composite materials and sandwich composite materials; see for example Refs. [1–5].

Although not visually apparent, low energy impact damage is found to be quite detrimental to the load bearing capacities of sandwich structures, underscoring the need for reliable damage detection techniques for composite sandwich structures. In recent years, structural health monitoring (SHM) using vibration based damage detection has been rapidly expanding and has shown to be a feasible approach for detecting and locating damage. The purpose of structural health monitoring systems is to provide information about the condition of a structure in terms of reliability and safety before the damage threatens the integrity of the structure. So the diagnosis of the damage in structural systems requires an identification of the location and type of damage, as well as the quantification of the degree of damage. Therefore, several techniques have been used to detect damage in structures. A detailed and comprehensive overview on the vibration based damage detection methods has been presented in Refs. [6–11]. The basic principle of vibration based damage detection can be explained as follows. Any structure can be considered as a dynamic system with stiffness, mass and damping. Once some damages emerge in the structures, the structural parameters will change, and the frequency response functions and modal parameters of the structural system will also change. This change of modal parameters can be taken as the signal of early damage occurrence in the structural system. Although vibration-based structural damage detection is a newly emergent research topic, its development can still be divided into traditional- and modern-type.

The traditional-type refers to detection method for structural damage by using only the structural characteristics, such as natural frequencies, modal damping, mode shapes, etc. These methods are among the earliest and most common, principally because they are simple to implement on any size structure. Structures can be excited by ambient energy, an external shaker or embedded actuators. Accelerometers and laser vibrometers can be used to monitor the structural dynamic responses. A variety of broadband excitation signals have been developed for making shaker measurements with FFT analyzers e.g., burst random, burst chirp, etc. Since the FFT provides a spectrum over a broad band of frequencies, using a broadband excitation signal makes the measurement of broadband spectral measurements much faster than using sine dwell or swept sine excitations [12]. Despite the fact that sine dwell or swept sine modal testing requires large acquisition times, but they have the capability of detecting non linear structural dynamic behavior unlike the broadband excitations [13]. Several modern techniques e.g., statistical process control, neural networks, advanced signal processing, genetic algorithm, wavelet analysis, etc., have been researched for detecting damage in composite materials, many of them showing the effectiveness of dynamic response measurements in monitoring the health of engineering structures [14–23]. These methods are generally classified as modern-type methods for damage detection.

Change in natural frequency is the most common parameter used in the identification of damage [24–26]. Various methods of damage detection that use natural frequency information are reported by salawu [27]. Kim and Hwang investigated the effect of the debonding extent on reduction in the flexural bending stiffness and on the natural frequency of honeycomb sandwich beams, and concluded that increasing face-layer debonding progressively reduces the flexural bending stiffness of the beams [28]. Lestari and Qiao extracted dynamic characteristics of a sandwich structure by collecting dynamic response data from piezoelectric smart sensors, in order to evaluate the location and magnitude of the damage [29]. Adams and Cawley localized damage in structure from measurements of natural frequencies [30]. Yam and Chang showed that with the increase in delamination size the natural frequency decreases, by artificially creating a crack and then vibrating the structure with the help of an embedded actuator [31]. Arkaduiz found that the presence of a self created delamination reduces the natural frequencies of a composite beam when harmonically excited [32]. Kim et al. also proposed a methodology to non-destructively locate and estimate the size of damage in structures using a few natural frequencies. They formulated a damage-localization algorithm in order to locate damage from changes in natural frequencies and a damage-sizing algorithm to estimate crack-size from natural frequency perturbation [33]. Khoo et al. employed different vibration techniques in order to locate damage in structures. They used resonant poles to identify the

modes, especially those modes that exhibit relatively large pole shifts are believed to be affected by damage [34]. Mattson et al. carried out damage detection based on residuals and discussed the phenomenon of false negatives. According to them, false negatives give no indication of damage when damage is present [35]. The advantage of using the change of structural natural frequency to detect damage is its convenient measurement and high accuracy. However the measurement of natural frequency cannot provide enough information for structural damage detection. Furthermore, the natural frequency is often not sensitive enough to initial damage in structures. Usually, this method can only ascertain existence of large damage, but may not be able to give the damage location because the structural damage in different location may cause the same frequency change.

However, in structures made of composite materials there seems to be a tendency to use damping as a damage indicator tool, as it tends to be more sensitive to damage than the stiffness variations. The introduction of damage into a material generally results in an increase of damping, which is related to energy dissipation during dynamic excitation. As friction is an energy dissipation mechanism, it is reasonable to assume that damping may be used for SHM, when this type of damage is concerned. Therefore, damping has also been proposed as a potentially sensitive and attractive damage indicator [36], though research works related to damping are fewer in number than those on natural frequency. The main sources of internal damping in a composite material arise from microplastic and viscoelastic phenomena in the matrix together with the interface effects between the matrix and the reinforcement [37]. The importance of damping as a parameter for damage detection is explained in scientific literature and has also been verified by the experimental results in this article. Zhang and Hartwig recommended damping in the evaluation of damage process which seemed more sensitive than the natural frequencies [38]. Gibson carried out vibration tests on composite specimens and found that for higher modes damping loss factor measurements are more significant than frequency measurements [39]. Similarly, Saravanos and Hopkins experimented on composite beams, and showed that the delamination has a more profound effect on modal damping than the natural frequencies [40]. Colakoglu showed that the damping factor increased with the number of fatigue cycles [41]. Richardson and Mannan found that the loss of stiffness in a structure corresponds to a decrease in natural frequency combined with an increase in damping [42].

The main motivation of the work presented in this article, is to carryout modal testing on intact and damaged sandwich beams by using both burst random and sine dwell testing in order to study the influence of impact damage and core-only damage on the global modal parameters (frequency and damping). The testing methodology used falls under the traditional-type vibration-based structural damage detection methods. In the end, a design of experiments is carried out on the experimental results, to determine that which modal testing method among burst random and sine dwell is more efficient for estimation in the presence of damping.

2. Material and specimen

In order to investigate the effect of impact and core-only damages on the modal parameters, honeycomb sandwich beams shall be used in this article. As this is a preliminary experimental study, therefore standard sandwich material like honeycomb is chosen for the instance. In future, this study will be extended to more complex sandwiches like entangled sandwich materials.

Resin-containing carbon-fiber/epoxy prepreg of T700/M21 is used to fabricate the skin materials [43]. The material is supplied by Hexcel composites, the physical properties are set out in Table 1. The upper and lower skins consist of four plies each with a stacking sequence of [0/90/90/0]. The thickness of each ply is 0.125 mm.

The core material is honeycomb and can be selected from a wide range of metallic and non-metallic honeycomb cores. The honeycomb sandwich beams in this article are made of Nomex-aramid honeycomb core (HRH 10) supplied by Hexcel composites [44]. The honeycomb core has a nominal cell size of 6.5 mm and a core thickness of 10 mm. Mechanical properties of the honeycomb core is listed in Table 2. The sandwich beam specimens are fabricated using an autoclave and an aluminum mold. The skin and the core are cured simultaneously in order to have an excellent bond. The final dimensions of the six identical honeycomb sandwich beams used in this article are $480 \times 50 \times 11\ \text{mm}^3$.

The vibration tests are carried out with two steel masses ($50 \times 25 \times 5\ \text{mm}^3$) attached at the ends [23,26]. The aim of putting these masses at the ends is to enhance the difference in the modal parameters between the undamaged and the damaged test specimens.

Table 1
Physical properties of carbon/epoxy prepreg T700/M21 used as skin material.

Young's modulus in fiber direction (E_1)	125 000 MPa
Young's modulus in transverse direction (E_1)	9000 MPa
Shear modulus (G_{12})	5000 MPa
Poisson ratio (ν_{12})	0.4
Volume density (ρ)	1550 kg/m^3

Table 2
Properties of honeycomb core (Hexel-aramid).

Cell size	6.5 mm
Density	31 kg/m^3
Compressive strength	0.896 MPa
Compressive modulus	75.8 MPa
Shear strength in longitudinal direction (σ_{xz})	0.65 MPa
Shear modulus in longitudinal direction (G_{xz})	29 MPa
Shear strength in width direction (σ_{yz})	0.31 MPa
Shear modulus in width direction (G_{yz})	13.8 MPa

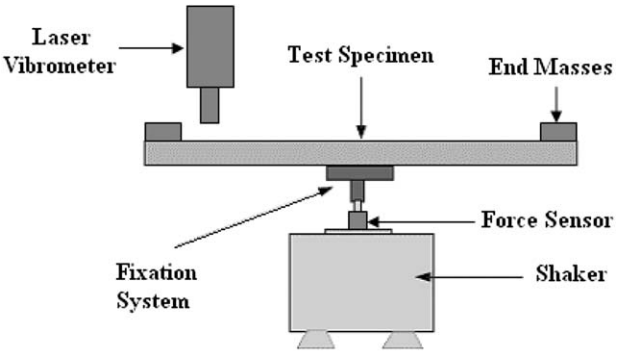

Fig. 1. Diagram of the experimental set-up.

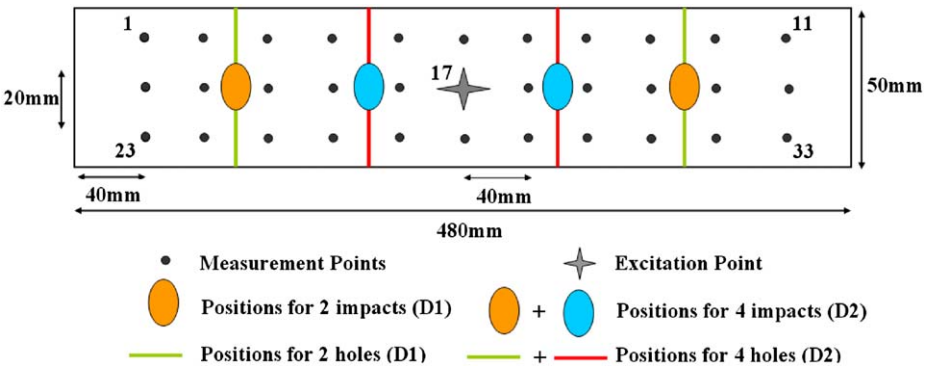

Fig. 2. Sandwich test specimen with location of impact damage, core-only damage (holes), excitation and measurement points.

3. Experimental methods

3.1. Vibration tests

The experimental equipment used for vibration testing is shown in Fig. 1. The experimental set-up is that of a free–free beam excited at its center, based on Oberst method [22]. The Oberst method states that a free–free beam excited at its center has the same dynamical behavior as that of a half length cantilever beam. The test specimen is placed at its center on a B&K force sensor (type 8200) which is then assembled on a shaker supplied by Prodera having a maximum force of 100 N. However the force sensor is not capable of measuring reliable response below 5 Hz. A fixation system is used to place the test specimens on the force sensor. The fixation is glued to the test specimens with a HBM X60 rapid adhesive. The response displacements are measured with the help of a non-contact and high precision Laser Vibrometer OFV-505 provided by Polytec. The shaker, force sensor and the laser vibrometer are manipulated with the help of a data acquisition system supplied by LMS Test Lab for burst random testing and Ideas Test (B&K) for sine dwell testing.

The center of the test specimens is excited at Point 17 as shown in Fig. 2. Each sandwich specimen is tested with two types of excitations i.e., burst random and sine dwell. For both the testing systems (LMS and B&K), the resolution is kept 0.25 Hz in order to obtain a good shape of the resonance peaks at low frequency range and to have a reliable comparison of modal parameters between the two systems. Response is measured at 33 points that are symmetrically spaced in three

rows along the length of the beam to have reliable identifiable mode shapes. The level of the excitation signal for both the excitations is chosen as 1 N which is kept fixed during all the vibration tests conducted in this paper. With the help of LMS by using burst random excitation, we have the advantage of having in quick time the overall dynamic (modal) response of our structure if we are mostly concerned with frequency and mode shapes. In addition, this broadband type of testing helps us identify the modes that we can use later on for sine-dwell testing. However if we need precise damping measurements then sine-dwell testing becomes inevitable but the problem with it is the lengthy acquisition times.

Burst random excitation is a broadband type excitation signal for which a 50 percent burst percentage is used. Normally burst random excitations are leakage free but after trying different window functions, it was found that by putting Hanning windows on both the excitation and response signals, better quality signals FRFs are obtained. The signal is averaged 10 times for each measurement point and the frequency band chosen is 0–2650 Hz.

Sine-dwell excitation is the discrete version of sine sweep. The frequency is not varied continuously, but is incremented by discrete amounts at discrete time points. The advantage of sine-dwell testing is its capability of detecting non linear structural dynamic behavior unlike the broadband excitations. As sine dwell testing requires larger acquisition times, so instead of studying the whole frequency band (0–2650 Hz), acquisition is carried out only around the first four bending modes previously identified by burst random testing by keeping the same resolution.

The modal parameters are extracted by Polymax and Polyreference, integrated in the data acquisition systems for burst random and sine-dwell testing respectively. The Polymax estimation method used by LMS acquisition system is a new non-iterative frequency domain parameter estimation method based on weighted least squares approach and uses measured FRFs as primary data. For the B&K system, one similar concept is used but in time-domain (Polyreference LSCE method), which typically require impulse responses (obtained as the inverse Fourier transforms of the FRFs) as primary data. Practically both of these methods work in similar fashion as follows:

- Firstly all the 33 FRFs are sort of superimposed along with a FRF sum. Limited frequency band estimation is then performed by taking each resonance separately.
- For accurate assessment of damping, a frequency interval of ± 20 Hz is chosen for each resonance peak for both Polymax and Polyreference, because by changing the frequency interval damping values can be affected.
- In the next step a stability diagram is constructed containing the poles i.e., frequency, damping information. For each mathematical model order, the poles are calculated from the estimated denominator coefficients of Eq. (3). The order of the mathematical model is shown on the right vertical end of the stability diagram. For reliable damping measurement, that value of pole should be chosen which displays a stable value for several model orders and if possible for each mode the value of poles should be chosen at the same model order to ensure that there is minimum uncertainty while comparing the damping values between different damage states.

One of the specific advantages of these two techniques lies in the very stable identification of the system poles and participation factors as a function of the specified system order, leading to easy-to-interpret stabilization diagrams. This implies a potential for automating the method and to apply it to "difficult" estimation cases such as high-order and/or highly damped systems with large modal overlap. As discussed previously, both Polymax and Polyreference are based on least-squares complex optimization methods, so both of them calculate the optimal pole value (frequency and damping) based on the 33 measurement points. We do not have access to the average values, variances or standard deviations for the 33 FRFs as the estimated modal parameters are the results of an optimized process.

The Ref. [47] explains these two estimators in detail.

So from the above discussion it can be said that both Polymax and Polyreference methods work in similar fashion, so the difference in the resulting modal parameters if it is the case, is due to the difference in excitations than due to the different estimation methods.

3.2. Impact tests

The six sandwich beams tested in this article are damaged in two different ways. The first four are damaged by drop weight impacts around the barely visible impact damage limit (BVID), in order to simulate damage by foreign impact objects such as stones or birds. The other two are damaged by piercing a hole all along the width in the honeycomb core by a hand drill, simulating mishandling during assembly and maintenance. The impact tests are carried out by a drop weight system as shown in Fig. 3, and a detailed cut away of the drop assembly is shown in Fig. 4.

The impactor tip has a hemispherical head with a diameter of 12.7 mm. A force sensor (type 9051A) provided by Kistler is placed between the impactor tip and the free falling mass of 2 kg. The impact velocity is measured with the help of an optic sensor. The combined weight of the impact head, freefalling mass, force sensor and the accelerometer is 2.03 kg. In the calculation of impact height, a factor of 1.1 is used to compensate for the losses due to friction between the guidance tube and the drop assembly. The size of the impact window is $80 \times 40\,mm^2$ which allows all the impact points to have the same boundary conditions and all the four ends are clamped. Further details on the impact test methodology of this drop tower can be found in the Refs. [3,26].

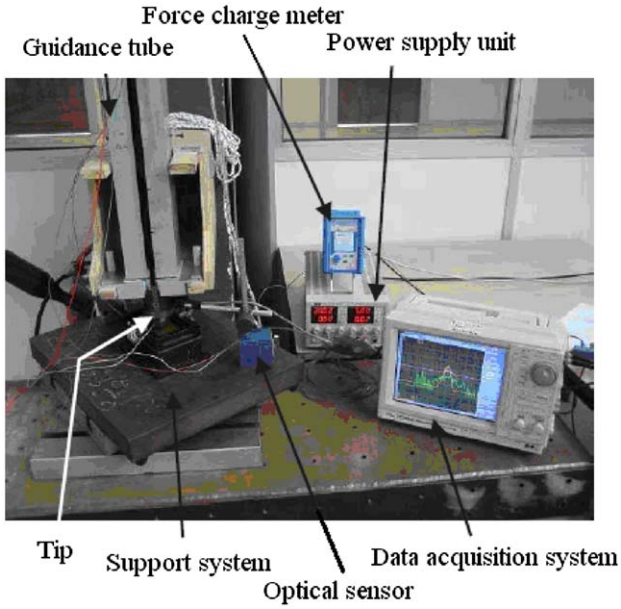

Fig. 3. Arrangement of the test equipment for the impact test.

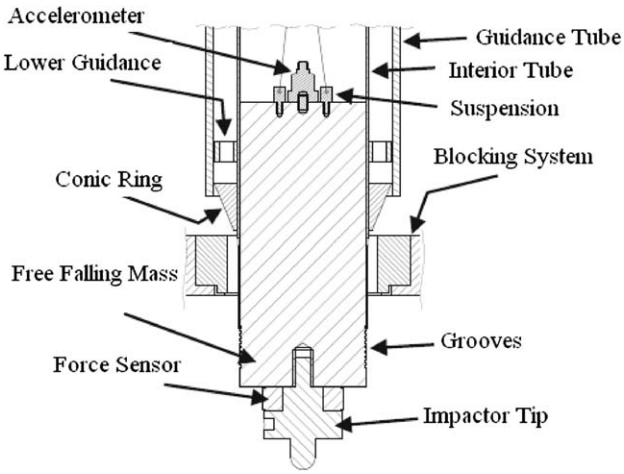

Fig. 4. Detailed cutaway of the drop assembly, the guidance tube and the blocking system.

In this article, a simple case with symmetric impacts is chosen. If satisfactory results are obtained, then asymmetric damage shall be studied in the future. Honeycomb sandwich beams are impacted by taking into account the barely visible impact damage limit (BVID). BVID corresponds to the formation of an indentation on the surface of the structure that can be detected by detailed visual inspection and can lead to high damage. In the aeronautical domain, BVID corresponds to an indentation of 0.3 mm after relaxation, aging, etc. (according to Airbus certifications). In this study, it is decided to take 0.6–0.8 mm of penetration depth as detectability criterion just after the impact [3] which corresponds to an indentation depth of approximately 0.3 mm by taking into account the above mentioned factors such as relaxation, aging, humidity, etc. The idea behind the impact tests is to damage the specimens below the BVID limit, in order to detect by vibration testing the damage that is not visible through naked eye. Four of the six sandwich beams are impacted symmetrically at four points with the same impact energy, as shown in Fig. 2. However in honeycomb sandwich beams, it is difficult to induce the same amount of damage at different points in the same specimen, even if it is impacted with the same energy i.e., impacting at the honeycomb cell center and at the corner leads to different damages. Therefore, it is not possible to have the same density of damage in honeycomb sandwich specimens at all the different impact points.

The first two honeycomb sandwich beams (H1 and H2) are impacted at 4J that produces a very small damage (not measurable by NDT methods) which is not visible on the surface. The reason for having the same impact energy for these

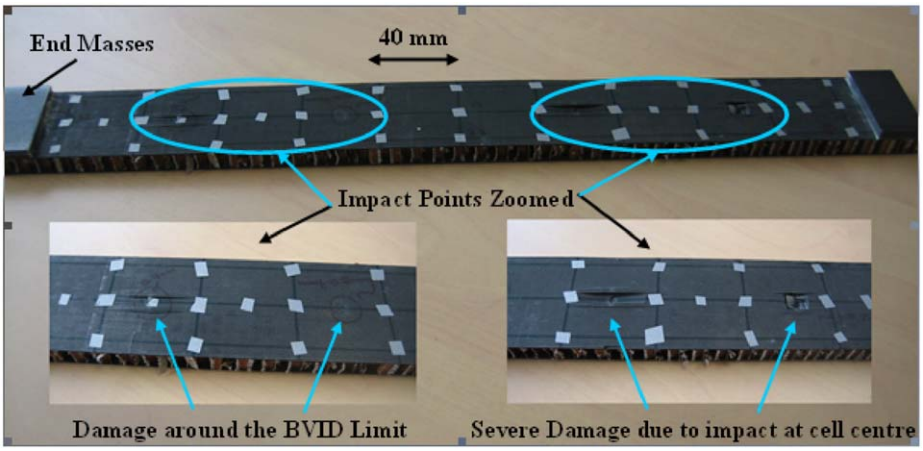

Fig. 5. Dispersion of damage at the four impact points in case of honeycomb beam H4 impacted at 8J.

Table 3
Impact parameters for honeycomb beams.

Honeycomb beam name	Energy of impact (J)	Height (mm)	Indentation just after impact (mm)	Velocity of impact measured (m/s)
H1 (without end-masses)	4	221.2	Very small damage	1.98
H2 (with end-masses)	4	221.2	Very small damage	1.98
H3 (with end-masses)	6	331.8	0.1–0.3	2.49
H4 (with end-masses)	8	442.3	0.7–3.0	2.83

two beams is to study the effect of end-masses i.e., H1 is without and H2 is with end-masses. The next honeycomb beam (H3) is impacted at 6J, which produces an indentation depth from 0.1 to 0.3 mm at the four impact points. However, the greatest dispersion in damage is seen in the honeycomb beam H4 which is impacted at 8J as shown in Fig. 5.

The damage depth for two impact points at one side of the beam is approximately 0.7 mm which corresponds to the BVID limit. But at the two impact points on the other end of the beam, the impactor head has induced severe damage due to impact at honeycomb cell center. This phenomenon introduces asymmetry in the beams and highlights the difficulty in inducing a global symmetric damage. The impact parameters for these four sandwich beams are listed in Table 3.

The data obtained during the drop weigh impact tests carried out on the honeycomb beams (H2–H4) is shown in Fig. 6. The impact test data for the honeycomb beams (H1 and H2) is similar as they are impacted with the same energy.

Four similar impacts have been performed on each specimen. However, in order to clarify these plots, only one impact test result for each specimen is plotted. All the impact curves presented in Fig. 6 are filtered at 15 kHz to avoid a free frequency of the impactor at about 20 kHz. These curves, representative of all performed impact tests, are very classic in the literature [4,5]. In Fig. 6a, the impact forces are drawn as a function of time. These curves are globally smooth and almost sinusoidal at low impact energy. The curves for all the three beams (H2–H4) show an important force signal fall followed by oscillations which is characteristic of delamination onset i.e., the appearance of first major damage in the sandwich beams. This is also evident in the force–displacement plot (Fig. 6b). The evolution of the peak force signal for the three beams (H2–H4) shows a logical increase with the increase in the impact energy.

As discussed previously, the second way of inducing damage is by piercing a hole all along the width in the honeycomb core by a hand drill as illustrated in Fig. 7. This type of damage can be referred to as core-only damage. In case of the honeycomb beams (H5) and (H6), approximately 5 and 10 mm diameter holes are pierced all along the width at the same positions as the impact points as shown in Fig. 2. For the 5 mm holes (Beam H5), some honeycomb material is present between the hole and the skins, however in case of 10 mm holes (Beam H6), no honeycomb material is present between the damage and the skin. The aim of inducing core-only damage is to check that whether this type of damage induces the same effect on the modal parameters as the impact damage. This will help us in future to develop algorithms based on modal parameters to detect these kinds of damages (impact and core-only damage) in sandwich structures.

The sandwich beams have three states. First one is the undamaged state (UD), the second is the damage state due to two impacts or two holes (D1) and the third is the damage state due to four impacts or four holes (D2). Vibration tests are carried out on the six sandwich beams after each of these three states. The effect of the impact damage and core-only

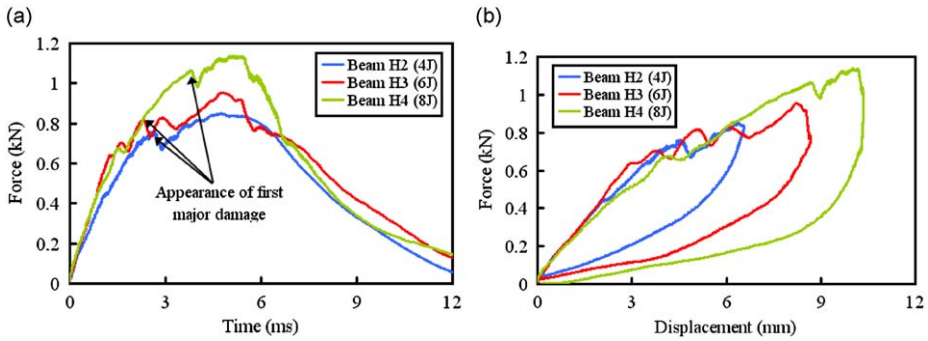

Fig. 6. Impact test data: (a) force-time; (b) force–displacement.

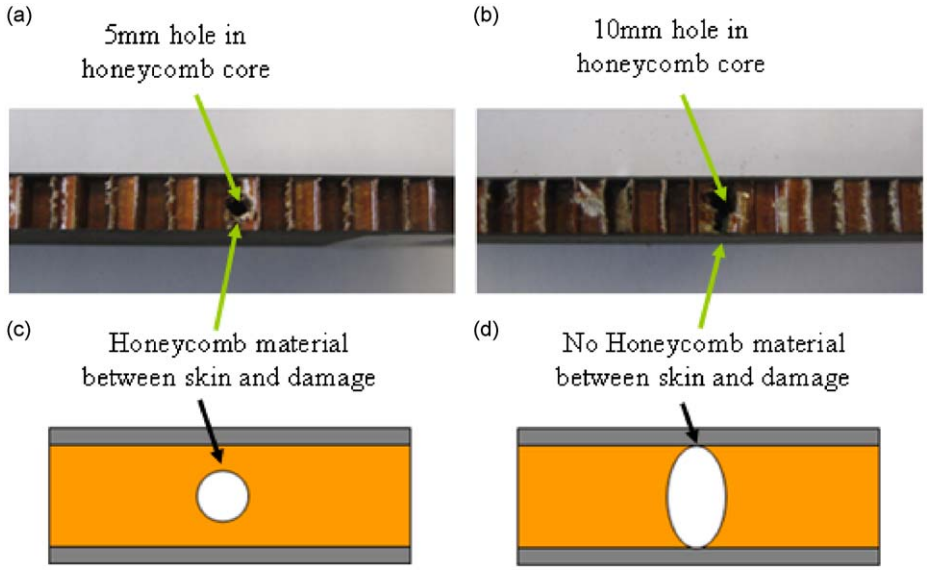

Fig. 7. Cross-section view of test beams showing the holes pierced in the honeycomb core all along the width: (a) 5 mm diameter hole for honeycomb beam H5; (b) approximately 10 mm diameter hole for honeycomb beam H6. Schematic view explaining presence and absence of material between the damage and the skin; (c) 5 mm diameter hole for honeycomb beam H5; (d) approximately 10 mm diameter hole for honeycomb beam H6.

damage on the modal parameters is studied in the following sections of this paper with the help of frequency and damping changes between the undamaged (UD) and the damaged states (D1 and D2) with the help of below equations:
Change in frequency between UD and D1:

$$(\Delta f) = \frac{f_{UD}(k) - f_{D1}(k)}{f_{UD}(k)} \tag{1}$$

Change in damping between UD and D1:

$$(\Delta \zeta) = \frac{\zeta_{D1}(k) - \zeta_{UD}(k)}{\zeta_{UD}(k)} \tag{2}$$

where $f_{UD}(k)$ is the damped natural frequency for the undamaged specimen for the kth mode and $f_{D1}(k)$ is the damped natural frequency for the specimen damaged at two impact points (D1) for the kth mode. Nomenclature in case of Eq. (2) is the same. Furthermore, in order to calculate the frequency and damping change ratios between UD and D2 the same procedure is used.

3.3. Tracking of poles for damage detection by modal analysis

Modal parameter estimation is a special case of system identification where the a priori model of the system is known to be in the form of modal parameters. The identification process consists of estimating the modal parameters from frequency

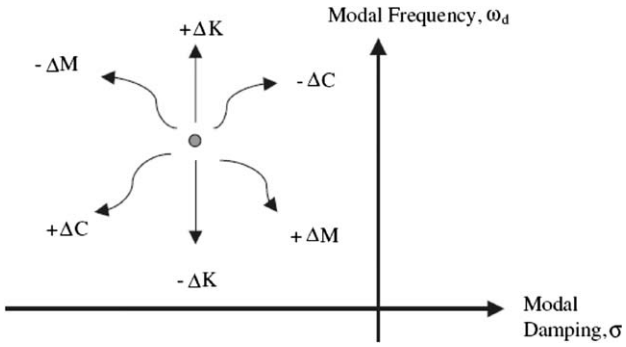

Fig. 8. Movement of pole due to mass stiffness and damping effect.

response function (FRF) measurements. Modal identification uses numerical techniques to separate the contributions of individual modes of vibration in measurements such as frequency response functions. Each term of the FRF matrix can be represented in terms of pole location and a mode shape. The FRF matrix model is represented mathematically by

$$[H(\omega)] = \sum_{k=1}^{\text{modes}} \left\{ \frac{[R(k)]}{(\mathrm{j}\omega(k) - p(k))} + \frac{[R(k)^*]}{(\mathrm{j}\omega(k) - p(k)^*)} \right\} \tag{3}$$

The numerator $R(k)$ is the residue of the FRF and is a function of the product between mode shape components at all points. The denominator gives the modal frequency and modal damping (second term in Eq. (3) is the complex conjugate term). The poles $p(k)$, are the roots that satisfy this equation and are related to modal frequency and damping as follows:

$$p(k) = -\sigma(k) + \mathrm{j}\omega(k) \tag{4}$$

The magnitude of each pole is the undamped natural frequency (ω_n). The undamped natural frequency (ω_n) and the modal damping (σ) are related to mass, stiffness and damping as follows: given by

$$\omega_n = \sqrt{\omega_d^2 + \sigma(k)^2} = \sqrt{\frac{K}{M}} \tag{5}$$

$$2\sigma(k) = \frac{C}{M} \tag{6}$$

The effect of physical properties on poles in the complex s-plane is illustrated in Fig. 8.

From Fig. 8, it can be observed that a change in stiffness affects only the frequency, while changes in mass and structural damping affect both modal damped frequency (ω_d) and modal damping (σ). For this study, the primary interest is to study the decrease in the modal damped frequency (ω_d) and the increase in modal damping (σ) due to damage in the sandwich specimens [45].

4. Results and discussion

4.1. Significance of end-masses

End-masses have been placed in case of composite laminate beams in scientific literature [26] in order to enhance the difference between the modal parameters for the undamaged and the damaged cases. But in case of sandwich composite beams, this phenomenon has to be verified. So in this article, vibration tests are carried out on honeycomb sandwich beams (H1 without end-masses) and (H2 with end-masses) to verify that whether in case of honeycomb sandwich beams the end-masses have as effect on modals parameters or not.

This study is conducted by studying the frequency and the damping change ratios presented in Table 4 between the undamaged (UD) and the two damaged cases (D1 and D2) for the honeycomb sandwich beams (H1 without end-masses) and (H2 with end-masses) for both burst random (BR) and sine dwell (SD) testing based on Eqs. (1) and (2). From Table 4, it can be said that on the whole the changes in frequency and damping ratios are more prominent in case of the beam H2 with end-masses. A closer examination of the results reveals that by adding end-masses, the damping ratios seem to be affected more as compared to the natural frequencies. A plausible explanation can be that the end-masses increase the effect of shearing forces which causes an increase in friction in the material, consequently leading to a higher change in damping ratios as compared to natural frequencies. Table 4 shows that by putting end-masses, the change in natural frequency (between the undamaged and the damaged cases) is increased by around 3 percent. However in case of damping ratios, this increase is as high as 93 percent. So clearly the damping ratios are more affected by the end-masses. It can also be noticed that the change in damping ratios is greater in case of sine dwell testing, because the damping ratio estimated by sine-dwell testing is always higher in case of the two damaged states (D1 and D2) as compared to the burst random

Table 4
Frequency and damping change ratios (%) between the undamaged (UD) and the two damaged states (D1 and D2) for the honeycomb sandwich beams (H1 without end-masses) and (H2 with end-masses) for both burst random (BR) and sine dwell (SD) testing.

Type of specimens	Between states	Natural frequency change ratios (%)							
		Mode 1		Mode 2		Mode 3		Mode 4	
		BR	SD	BR	SD	BR	SD	BR	SD
H1 (4J)	UD and D1	5.9	6.2	9.1	9.6	10.7	10.8	8.3	8.4
No end-masses	UD and D2	12.2	12.8	16.0	16.4	14.3	14.5	14.9	15.7
H2 (4J)	UD and D1	8.3	8.7	9.5	9.0	13.5	13.6	12.7	12.6
With end-masses	UD and D2	13.6	14.2	19.5	20.2	16.1	16.7	17.7	17.7
		Damping change ratios (%)							
		BR	SD	BR	SD	BR	SD	BR	SD
H1 (4J)	UD and D1	14.9	124.6	38.2	125.3	21.5	73.1	6.9	33.7
No end-masses	UD and D2	132.5	153.4	56.2	188.7	19.8	153.2	17.7	40.2
H2 (4J)	UD and D1	21.1	4.3	92.5	159.9	44.8	102.9	12.1	68.5
With end-masses	UD and D2	574.5	752.7	127.0	294.4	64.9	135.8	−10.9	242.7

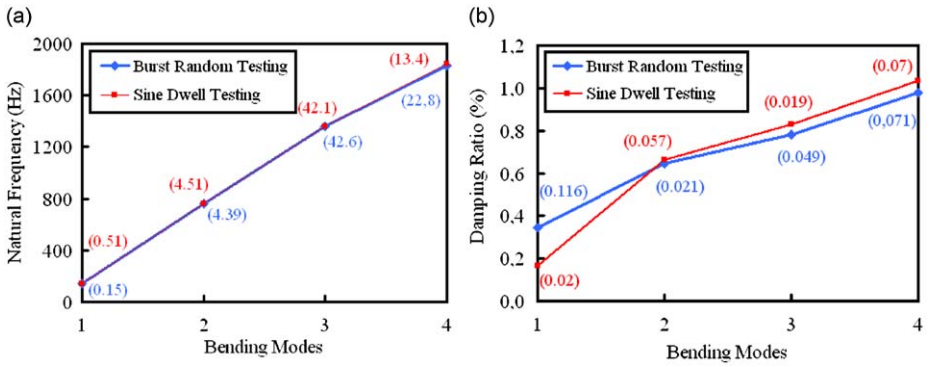

Fig. 9. Average values of modal parameters: (a) natural frequency; (b) damping ratio for the first four bending modes for the five honeycomb sandwich beams (H2–H6) with both burst random and sine dwell testing. The standard deviation of the modal parameters for each mode is represented in black (blue) for burst random and in grey (red) for sine dwell testing. (For interpretation of the references to colour in this figure legend, the reader is referred to the web version of this article.)

testing (also seen in Fig. 12 and Table 6). Therefore, the rest of the honeycomb sandwich beams (H2–H6) except beam H1 in this article have been tested with end-masses.

4.2. Estimation of modal parameters at the undamaged state

Theoretically all the beams at the undamaged state should possess similar natural frequency and damping values, but due to fabrication anomalies there can be some dispersion. As all the beams are at the undamaged state and the testing parameters have been kept the same for all beams so the authors think that it is logical to compare the average natural frequency and average damping ratio values for all the beams for the first four bending modes with their respective standard deviation values to give an idea about the dispersion at the undamaged state.

In this section the modal parameters of the five honeycomb sandwich beams with end-masses (H2–H6) are discussed. In order to have a clear picture, the average values of natural frequencies and damping ratios for the first four bending modes of these five beams (H2–H6) with both burst random and sine dwell testing are plotted in Fig. 9. The standard deviation associated with each average value is also represented for both burst random and sine dwell testing. In case of natural frequencies, the two types of testing, give similar results at the undamaged states as shown by the standard deviation values. However the dispersion at the 3rd bending mode for the natural frequency is a bit on the higher side, which is due to the fact that the beam H5 at the 3rd bending mode has a natural frequency of 1429 Hz whereas the average for the other four beams is 1338 Hz. This dispersion in natural frequency at Mode 3 occurs in case of both of testings. This anomaly outlines the inherent possibility of false negatives which can arise due to boundary conditions and gives no indication of damage when it is present as discussed in the Ref. [35].

In case of damping ratios, the results at the undamaged state give a good comparison as well for the two types of testings with small standard deviation values. However the exception in case of the damping ratios is the 1st bending mode for burst random testing which has a high standard deviation value of 0.116 (Fig. 9b). This is because of the honeycomb beam H2, which has a damping ratio of 0.161 percent for the 1st bending mode, whereas the average damping ratio for the other four beams estimated by burst random testing is 0.389 percent. This dispersion is not present in case of sine dwell testing, so this result gives us a first indication that the sine dwell testing might be better suited for damping estimation.

4.3. *Effect of impact damage on modal parameters*

The effect of impact damage on the honeycomb sandwich beams is studied with the help of modal parameter changes for the first four bending modes as they have the largest amplitudes for the type of test configuration presented in this article. The variation of natural frequency and damping ratio due to impact damage is studied for the honeycomb beams (H2–H4) with end-masses. Frequency and damping ratios are the global parameters of the specimen, and are extracted from high quality measurements carried out on the 33 measurement points. The modal parameters (natural frequency and damping) help in monitoring globally the health of a specimen. For the first four bending modes, the variation of damped natural frequency as a function of the undamaged (UD) and the two damage states (D1 and D2) for the honeycomb beams (H2–H4) for both burst random (BR) and sine-dwell (SD) testings is presented in Fig. 10.

As discussed before in Section 4.1, that damage in the specimens prompts a decrease in natural frequencies. So from Fig. 10, it is clear that the decrease in the natural frequencies for the three honeycomb beams is more prominent in case of the beam H4 impacted at 8J. In case of natural frequencies, both burst random and sine-dwell testing give similar results. But the interesting fact is that, even for beam H2 impacted at 4J which does not produce a visible damage on the surface, the average change in frequency for the first four bending modes between the undamaged and the damaged cases is 14 percent, which proves that the beam H2 has a notable loss of rigidity without any signs of damage on the beam surface. It is particularly in these cases that vibration testing becomes a very useful tool for structural health monitoring. It is noticed that in case of honeycomb beams H3 and H4 impacted at 6 and 8J respectively, the level of damage is not the same on both sides of the beams as it depends on whether the honeycomb cell center or corner is impacted as discussed previously and shown in Fig. 5. So this asymmetric damage leads to distortion of the resonance peaks or the appearance of twin peaks instead of one. This is evident in Fig. 11, which shows a comparison of the sum of the frequency response functions (FRF), estimated by burst random testing, for the honeycomb sandwich beams (H2–H4) for the undamaged case (UD), damaged at 2 points (D1) and damaged at 4 points (D2) for the 2nd bending mode. The sum of the FRF can be compared as for each sandwich beam 33 symmetric measurement points have been chosen that are symmetric on both sides of the two major axes of symmetry.

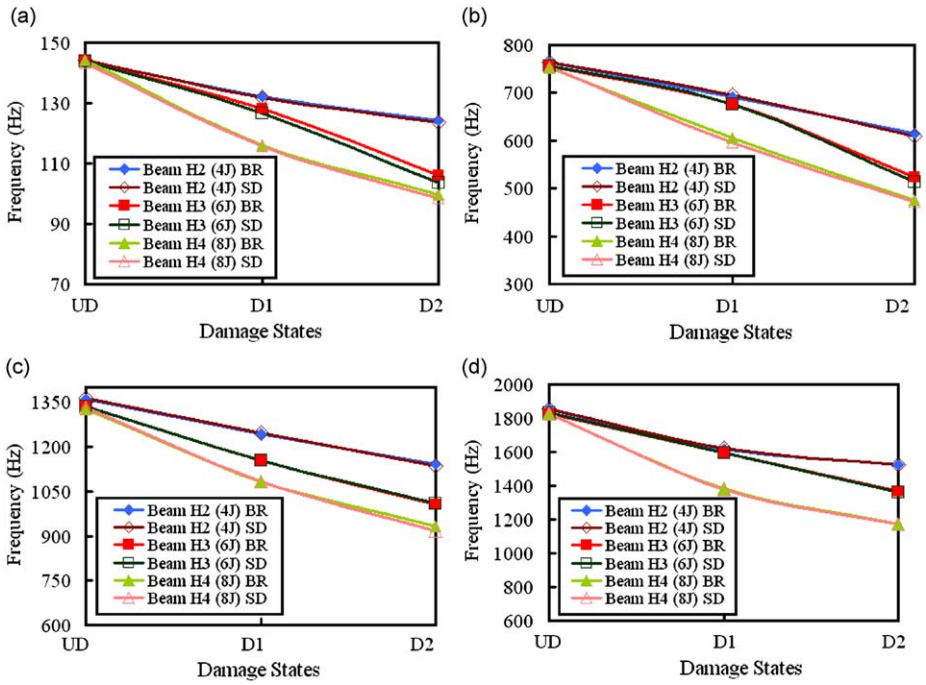

Fig. 10. Variation of damped natural frequencies with damage states for: (a) 1st bending mode; (b) 2nd bending mode; (c) 3rd bending mode; (d) 4th bending mode: UD is undamaged state, D1 is damaged at 2 impact points and D2 is damaged at 4 impact points, for the honeycomb beams (H2–H4) for both burst random (BR) and sine-dwell (SD) testing.

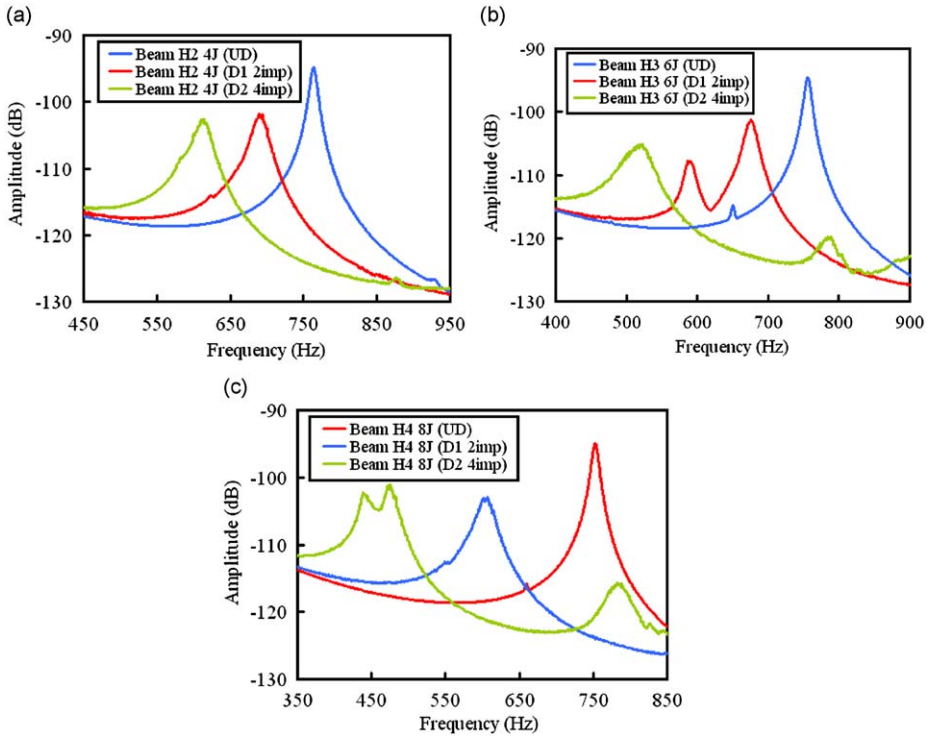

Fig. 11. Comparison of the sum of the frequency response functions estimated by burst random testing for the undamaged case (UD), damaged at 2 points (D1) and damaged at 4 points (D2) for the 2nd bending mode for honeycomb beams: (a) H2 damaged at 4J; (b) H3 damaged at 6J; (c) H4 damaged at 8J.

Fig. 11a shows that the resonance peaks for the beam H2 impacted at 4J are pretty much intact even for the damaged cases, showing that on the whole the beam is lightly damaged. But for the beams H3 and H4, as the damage level increases and with the addition of the asymmetric distribution of damage as discussed previously, the shape of peaks becomes distorted. This distortion of peaks does not affect the estimation of natural frequencies as such, as shown in Fig. 10 i.e., both burst random and sine-dwell testing give similar natural frequency results in the presence of damage. However, for the estimation of damping ratios for the damage states D1 and D2, there is a notable difference between the results of burst random and sine dwell testing as shown in Fig. 12.

It can be seen in Fig. 12 that in general the damping increases with the increase in damage in the sandwich beams. However, in case of burst random testing, for the beam H2 for the 4th bending mode (Fig. 12d) and for the beam H4 for the 1st bending mode (Fig. 12a) the damping does not increase with damage. However sine dwell testing shows a logical increase of damping for these beams. Furthermore, the estimation of damping by sine-dwell testing for the damage state (D2) is always notably higher as compared to burst random testing with the exception of the beam H3 for the 1st bending mode. It confirms the fact that sine dwell testing is more capable of detecting non linear structural dynamic behavior (due to accumulation of high damage as in state D2) unlike the broadband excitations [13].

4.4. *Effect of core-only damage on modal parameters*

As discussed previously, in case of the honeycomb beams (H5) and (H6), approximately 5 and 10 mm diameter holes are pierced all along the width at the same positions as the impact points. The aim of inducing core-only damage is to see that whether this type of damage induces the same effect on the modal parameters as the impact damage. The effect of core-only damage on the natural frequency and damping is studied similarly as the impact damage and is shown in Figs. 13 and 14.

Fig. 13 shows that the core-only damage induces a smaller change in natural frequencies as compared to the impact damage. The change in frequencies between the damaged states and the undamaged state is below 7 percent for both the honeycomb beams H5 and H6 as shown by the frequency change ratios in Table 5. Both burst random and sine-dwell testing give relatively similar results for natural frequencies with the exception of beam H5 for the 4th bending mode. It is interesting to note that there is no remarkable change in damping ratios for the beams H5 and H6 in the presence of core-only damage, with the exception of the damping for the 1st bending mode estimated by burst random testing for both beams H5 and H6. Whether the damping increases or decreases with damage, the change in damping ratio is generally very small between the undamaged (UD) and the damaged cases (D1 and D2). So it can be concluded that the core-only damage does not reduce much the stiffness of the honeycomb sandwich beams as compared to the impact damage. As the change

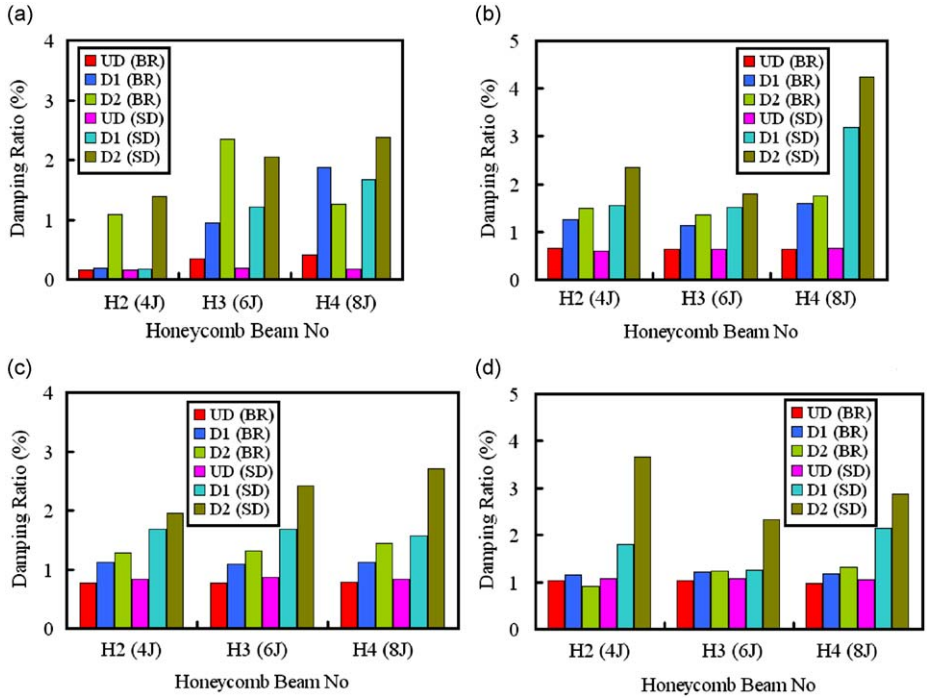

Fig. 12. Variation of damping ratio with damage states for: (a) 1st bending mode; (b) 2nd bending mode; (c) 3rd bending mode; (d) 4th bending mode: UD is undamaged state, D1 is damaged at 2 impact points and D2 is damaged at 4 impact points, for the honeycomb beams (H2–H4) for both burst random (BR) and sine-dwell (SD) testing.

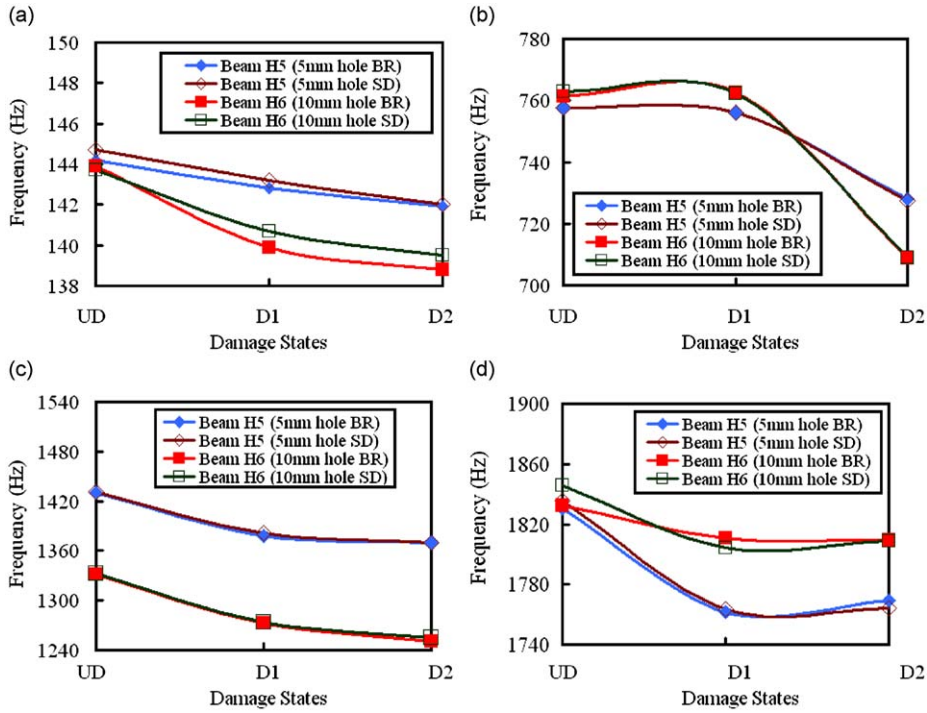

Fig. 13. Variation of damped natural frequencies with damage states for: (a) 1st bending mode; (b) 2nd bending mode; (c) 3rd bending mode; (d) 4th bending mode: UD is undamaged state, D1 is damaged at 2 points of impact and D2 is damaged at 4 points of impacts, for the honeycomb beams (H5 and H6) for both burst random (BR) and sine-dwell (SD) testing.

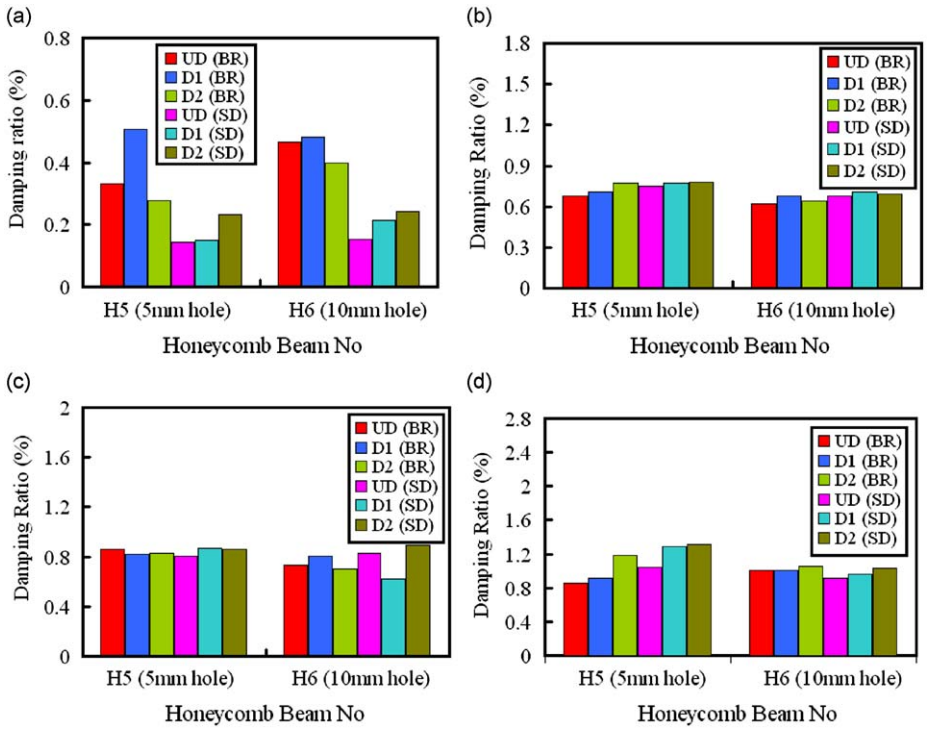

Fig. 14. Variation of damping ratios with damage states for: (a) 1st bending mode; (b) 2nd bending mode; (c) 3rd bending mode; (d) 4th bending mode: UD is undamaged state, D1 is damaged at 2 points of impact and D2 is damaged at 4 points of impacts, for the honeycomb beams (H5 and H6) for both burst random (BR) and sine-dwell (SD) testing.

Table 5
Frequency change ratios between the undamaged (UD) and the two damaged states (D1 and D2) for the impact damaged honeycomb beams (H3, H4) and the core-only damaged honeycomb beams (H5, H6) for both burst random (BR) and sine-dwell (SD) testing.

Type of specimens	Between states	Mode 1		Mode 2		Mode 3		Mode 4	
		BR	SD	BR	SD	BR	SD	BR	SD
H3 (6J)	UD and D1	10.9	11.9	10.5	10.7	13.6	13.6	12.7	12.9
	UD and D2	26.3	28.0	30.8	32.1	24.5	24.4	25.3	25.6
H4 (8J)	UD and D1	19.4	19.3	19.5	20.9	18.3	18.6	24.3	24.5
BVID	UD and D2	30.8	31.3	36.7	37.3	29.7	31.0	35.7	35.8
H5	UD and D1	0.9	1.0	0.2	0.2	3.5	3.4	3.7	3.9
5 mm hole	UD and D2	1.6	1.8	3.8	3.9	4.1	4.2	3.3	3.9
H6	UD and D1	2.7	2.0	−0.1	0.0	4.4	4.4	1.1	2.2
10 mm hole	UD and D2	3.5	2.9	6.9	7.0	6.0	5.8	1.2	1.9

in modal parameters is slight for the core-only damage, so it shall be more difficult to carryout core-only damage detection with the help of modal parameter changes.

The effect of impact and core-only damage on the frequencies and damping ratios can be further elaborated by studying the frequency and the damping change ratios between the undamaged (UD) and the damaged cases (D1 and D2) for the impact damaged beams H3 and H4 and for the core-only damaged beams H5 and H6 in Tables 5 and 6. Same procedure as explained in Section 4.2 is followed. It can be clearly seen that the change in modal parameters is by far more prominent in case of the impact damaged beams (H3 and H4). Furthermore, the results in Tables 5 and 6 underline the fact that the damping change ratios are more prominent than the frequency change ratios. The maximum damping change ratio is 968 percent whereas the maximum frequency change ratio is 38 percent. As discussed previously, the damping change ratio estimated by sine-dwell testing is higher as compared to burst random testing. It can be concluded from the above results that damping seems more sensitive to damage than the natural frequency variations in case of honeycomb sandwich beams. So it is reasonable to assume that damping may be used instead of natural frequency as a damage indicator tool for structural health monitoring purposes. However, the fact that damping is a parameter that is relatively difficult to estimate as compared to natural frequency has to be taken into account [46].

Table 6
Damping change ratios between the undamaged (UD) and the two damaged states (D1 and D2) for the impact damaged honeycomb beams (H3, H4) and the core-only damaged honeycomb beams (H5, H6) for both burst random (BR) and sine-dwell (SD) testing.

Type of specimens	Between states	Mode 1		Mode 2		Mode 3		Mode 4	
		BR	SD	BR	SD	BR	SD	BR	SD
H3 (6J)	UD and D1	175.1	531.7	78.4	137.2	41.8	95.8	18.4	16.6
	UD and D2	877.1	968.2	113.6	179.7	72.7	181.5	19.8	23.2
H4 (8J)	UD and D1	348.4	839.5	146.7	388.2	42.8	88.3	22.1	104.6
BVID	UD and D2	200.7	1245	172.6	549.4	83.2	226.6	35.6	172.2
H5	UD and D1	53.4	6.3	3.8	3.0	−5.1	7.8	6.4	22.7
5 mm hole	UD and D2	−16.3	64.7	14.1	4.5	−3.4	6.8	38.1	25.2
H6	UD and D1	3.22	40.1	9.3	4.2	10.5	−25.2	0.1	4.8
10 mm hole	UD and D2	−14.8	59.8	2.5	1.7	−3.7	7.4	5.6	12.6

Table 7
Comparison of natural frequency and damping ratios for both up and down sine-dwell frequency directions for the honeycomb beams H3 and H4 for the damage state (D2).

Type of specimens	Sine dwell direction	Natural frequency (Hz)				Damping ratio (%)			
		Mode1	Mode 2	Mode 3	Mode 4	Mode1	Mode 2	Mode 3	Mode 4
H3 (6J)	Up	97.5	499.5	1010.1	1374.0	2.05	1.79	2.42	1.33
D2 (4imp)	Down	98.8	499.1	1010.2	1378.6	2.73	1.83	2.36	1.00
H4 (8J)	Up	98.4	471.9	918.4	1172.2	2.38	4.24	2.71	2.86
D2 (4imp)	Down	98.1	467.7	921.8	1175.7	2.46	4.63	2.99	2.90

4.5. Effect of sine-dwell frequency direction on modal parameters

The aim of carrying out sine dwell testing in both up and down frequency directions is to be able to detect structural non-linearities in the damaged honeycomb beams. In literature it has been shown that frequency response functions (FRF) vary for the different sweep directions [13]. In this article, the effect of sweep directions is studied only for the beams with the highest level of damage i.e., impact damaged beams H3 and H4 for the damage state (D2) as presented in Table 7.

Table 7 shows the presence of nonlinear behavior in the honeycombs beams H3 and H4, as the natural frequencies and damping ratios show a slight discrepancy when tested in the increasing and decreasing frequency order. This is also shown graphically in Fig. 15 by plotting the frequency response functions from sine-dwell sweeps upwards and downwards in frequency. It is observed that in the presence of non-linearity, there is always a change in amplitude coupled with a slight shift in frequencies.

5. Design of experiments (DOE)

Design of experiments (DOE) is a powerful analysis tool for highlighting the influence of key parameters that affect an experimental process and the output of that process [45]. This study is carried out on the modal parameters (natural frequency and damping ratio) of the three impact damaged sandwich beams with end-masses (H2–H4) tested by both burst random and sine-dwell testing. The aim is to find out that which testing method gives a more logical estimation of damping in the presence of damage i.e., damping increases with the increase of damage in the specimen [42]. The design of experiments shall also help us identify the factors which have the most significant effect on the experimentally obtained modal parameters.

The two factors chosen for the design of experiments are the energy of impact (IE) and the density of damage (DD). For the energy of impact there are three levels (4, 6 and 8J) and for the density of damage there are also three levels (the undamaged state (UD), damage at 2 impact points (D1) and damage at 4 impact point (D2)). By keeping in view the levels of the two factors, a full factorial design is chosen. The linear regression model associated with the full factorial design, based on the two variables discussed above is expressed as follows:

$$Y = a_0 + a_1 \cdot (\mathrm{IE}) + a_2 \cdot (\mathrm{DD}) + a_3 \cdot (\mathrm{IE}) \cdot (\mathrm{DD}) + E \tag{7}$$

In Eq. (7), coefficients represent model constants (a_i) that are the contribution of independent variables on the response. E is the random error term representing the effects of uncontrolled variables, i.e., not included in the model. The model constants (a_i) are determined by multi-linear regression analysis and are assumed to be normally distributed. The error is assumed to be random and normally distributed. These constants (a_i) are obtained with 90 percent confidence level.

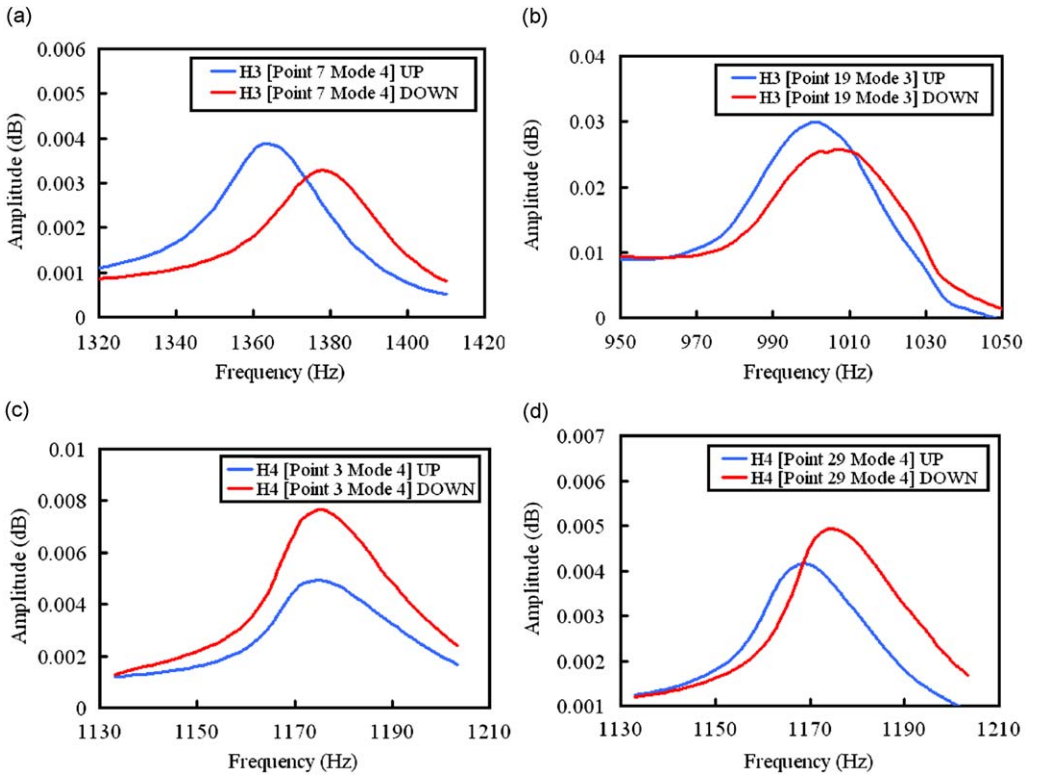

Fig. 15. FRFs from sine-dwell sweeps upwards and downwards in frequency honeycomb beams: (a) H3 Point 7 mode 4; (b) H3 Point 19 mode 3; (c) H4 Point 3 mode 4; (d) H4 Point 29 mode 4.

Table 8
Coefficients and t ratios for the natural frequencies (Hz) estimated by burst random testing.

Term	Mode 1		Mode 2		Mode 3		Mode 4	
	Constants (a_i)	t ratio	Constants (a_i)	t ratio	Constants (a_i)	t ratio	Constants (a_i)	t ratio
IE	−3.35	−5.53	−19.59	−6.42	−33.46	−7.49	−51.19	−4.55
DD	−8.51	−14.05	−54.98	−18.02	−78.49	−17.57	−120.4	−10.70
IE × DD	−1.55	−4.18	−7.95	−4.25	−10.99	−4.02	−20.21	−2.94

The significance of each variable on a given response (modal parameters in our case) is investigated using t test values based on student's distribution. The t ratio is the ratio of the parameter estimate (constants) to its standard deviation. A t ratio greater than 2 in absolute value is a common rule of thumb for judging significance of the variable. The derived constants (a_i) and t ratios for the natural frequencies and the damping ratios estimated by burst random testing are presented in Tables 8 and 9. Negative values of the model constants and t ratios indicate that the response decreases with the increase in the value of the parameter. In our case, this is most of the times true for the natural frequencies as they decrease with the increase in damage in the specimens.

By comparing the t ratios for the energy of impact (IE) and the density of damage (DD) in Tables 8 and 9, it can be seen that the density of damage (DD) has a more significant effect on the modal parameters than the impact energy (IE) for the first four bending modes. The second order interaction term (IE × DD) is more significant in case of the natural frequencies as compared to the damping ratios. Similar results are observed in case of sine-dwell testing. The design of experiment results based on the modal parameters estimated by sine-dwell testing are laid out in Tables 10 and 11.

Sine-dwell testing also proves the significance of density of damage (DD) as the parameter that has the most significant effect on the results. If the t ratios for the damping ratios estimated by burst random and sine-dwell testing are compared in Tables 9 and 11, it can be seen that the two factors (IE and DD) have higher t ratios in case of the damping ratios estimated by sine-dwell testing. So it can be concluded that sine-dwell testing gives more reliable estimation of damping in the presence of damage as compared to burst random testing. Although the main disadvantage of sine-dwell testing is the

Table 9
Coefficients and t ratios for damping ratios (%) estimated by burst random testing.

Term	Mode 1		Mode 2		Mode 3		Mode 4	
	Constants (a_i)	t ratio	Constants (a_i)	t ratio	Constants (a_i)	t ratio	Constants (a_i)	t ratio
IE	0.175	1.49	0.049	1.11	0.015	1.74	0.029	1.62
DD	0.313	2.68	0.541	3.83	0.381	13.58	0.036	2.01
IE × DD	−0.005	−0.08	0.017	0.65	0.009	1.76	0.028	2.58

Table 10
Coefficients and t ratios for the natural frequencies (Hz) estimated by sine-dwell testing.

Term	Mode 1		Mode 2		Mode 3		Mode 4	
	Constants (a_i)	t ratio	Constants (a_i)	t ratio	Constants (a_i)	t ratio	Constants (a_i)	t ratio
IE	−3.52	−3.36	−20.7	−4.77	−34.1	−8.95	−51.98	−4.63
DD	−9.33	−8.91	−57.8	−13.30	−80.6	−21.14	−121.3	−10.8
IE × DD	−1.52	−2.38	−7.93	−2.98	−11.5	−4.94	−20.3	−2.96

Table 11
Coefficients and t ratios for damping ratios (%) estimated by sine-dwell testing.

Term	Mode 1		Mode 2		Mode 3		Mode 4	
	Constants (a_i)	t ratio	Constants (a_i)	t ratio	Constants (a_i)	t ratio	Constants (a_i)	t ratio
IE	0.208	3.57	0.300	2.13	0.053	1.90	−0.039	−0.39
DD	0.441	7.56	0.221	5.02	0.142	16.09	0.472	4.59
IE × DD	0.061	1.71	0.114	1.33	0.047	2.75	−0.049	−0.78

lengthy acquisition times as compared to broadband excitations, but if quality damping estimations are required then sine-dwell excitation based vibration testing becomes indispensable.

6. Conclusion

Vibration tests have been carried out on pristine and damaged honeycomb sandwich beams using burst random and sine dwell excitations in order to compare that which testing method gives a more logical estimation of damping in the presence of damage, because damping is much harder to estimate as compared to natural frequency. Vibration tests are carried out by placing steel masses at the two ends of the sandwich beams in order to enhance the shift between the modal parameters between the undamaged and the damaged cases. The six sandwich beams tested in this article are damaged in two different ways. The first four are damaged by drop weight impacts around the barely visible impact damage limit (BVID), in order to simulate damage by foreign impact objects such as stones or birds. The other two are damaged by piercing a hole all along the width in the honeycomb core by a hand drill (core-only damage), simulating mishandling during assembly and maintenance. Results show that with the accumulation of damage in the specimens, there is a decrease in natural frequency accompanied by an increase in damping ratio. The impact of core-only damage seems feeble on the modal parameters as compared to impact damage. Furthermore, damping seems to be more sensitive to damage than the natural frequency. So it is reasonable to assume that damping may be used instead of natural frequency as a damage indicator tool for structural health monitoring purposes. Presence of non-linearity in the impacted sandwich beams is proved by carrying out sine-dwell testing upwards and downwards in frequency. It is observed that in the presence of non-linearity, there is always a change in amplitude coupled with a slight shift in frequencies in the FRFs. Design of experiments carried out on the extracted modal parameters show highlighted density of damage as the factor having the most significant effect on the modal parameters, and prove that sine-dwell excitation based modal testing gives more reliable estimation of damping in the presence of damage as compared to burst random testing. In future similar vibration tests shall be carried out with different excitation levels and asymmetric impacts in order to study their effects on modal parameters.

Acknowledgments

The authors gratefully thank professor B. Castanié from Université de Toulouse and research project student Hanno Niemann from TU Braunschweig for their technical support during the experimental work.

References

[1] P.M. Schubel, J.J. Luo, I.M. Daniel, Impact and post impact behaviour of composite sandwich panels, *Composites Part A* 38 (2007) 1051–1057.
[2] J.P. Dear, H. Lee, S.A. Brown, Impact damage processes in composite sheet and sandwich honeycomb materials, *International Journal of Impact Engineering* 32 (2005) 130–154.
[3] S. Petit, C. Bouvet, A. Bergerot, J.J. Barrau, Impact and compression after impact experimental study of a composite laminate with a cork thermal shield, *Composites Science and Technology* 67 (2007) 3286–3299.
[4] P.H. Bull, F. Edgren, Compressive strength after impact of CFRP-foam core sandwich panels in marine applications, *Composites Part B* 35 (6–8) (2004) 535–541.
[5] S. Abrate, *Impact on Composite Structures*, Cambridge University Press, Cambridge, 1988.
[6] S.W. Doebling, C.R. Farrar, M.B. Prime, D.W. Shevitz, Damage identification and health monitoring of structural and mechanical systems from changes in their vibration characteristics: a literature review. *Research Report LA-13070-MS ESA-EA Los Alamos National Laboratory*, 1996.
[7] S.W. Doebling, C.R. Farrar, M.B. Prime, A summary review of vibration-based damage identification methods, *Shock and Vibration Digest* 30 (1998) 91–105.
[8] Y.J. Yan, L. Cheng, Z.Y. Wu, L.H. Yam, Development in vibration-based structural damage detection technique, *Mechanical Systems and Signal Processing* 21 (2007) 2198–2211.
[9] H. Sohn, C.R. Farrar, F.M. Hemez, D. Shunk, D.W. Stinemates, B.R. Nadler, A review of structural health monitoring literature: (1996–2001) *Los Alamos National Laboratory Report LA-13976-MS*.
[10] E.P. Carden, P. Fanning, Vibration based condition monitoring: a review, *Structural Health Monitoring* 3 (4) (2004) 355–377.
[11] H. Van der Auweraer, International research projects on structural damage detection, *Damage Assessment of Structures Key Engineering Materials* 204 (2) (2001) 97–112.
[12] B.J. Schwarz, M.H. Richardson, *Experimental Modal Analysis*, CSI Reliability week, Orlando, FL, 1999.
[13] G. Gloth, M. Sinapius, Influence and characterisation of weak non-linearities in swept-sine modal testing, *Aerospace Science and Technology* 8 (2004) 111–120.
[14] M.L. Fugate, H. Sohn, C.R. Farrar, Vibration-based damage detection using statistical process control, *Mechanical Systems and Signal Processing* 15 (4) (2001) 707–721.
[15] K. Waldron, A. Ghoshal, M.J. Schulz, M.J. Sundaresan, F. Ferguson, P.F. Pai, J.H. Chung, Damage detection using finite elements and laser operational deflection shapes, *Journal of Finite Elements in Analysis and Design* 38 (2002) 193–226.
[16] M.J. Sundaresan, P.F. Pai, A. Ghoshal, M.J. Schulz, F. Ferguson, J. Chung, Methods of distributed sensing for health monitoring of composite material structures, *Composites A Journal* 32 (2001) 1357–1374.
[17] J.R. LeClerc, K. Worden, W.J. Staszewski, J. Haywood, Impact detection in an aircraft composite panel—a neural network approach, *Journal of Sound and Vibration* 299 (3) (2007) 672–682.
[18] H.T. Banks, D.J. Inman, D.J. Leo, Y. Wang, An experimentally validated damage detection theory in smart structures, *Journal of Sound and Vibration* 191 (1996) 859–880.
[19] M. Krawczuk, W. Ostachowicz, Identification of delamination in composite beams by genetic algorithm, *Science and Engineering of Composite Materials* 10 (2) (2002) 147–155.
[20] Y.J. Yan, L.H. Yam, Online detection of crack damage in composite plates using embedded piezoelectric actuators/sensors and wavelet analysis, *Composite Structures* 58 (1) (2002) 29–38.
[21] C.Y. Kao, S.L. Hung, Detection of structural damage via free vibration responses generated by approximating artificial neural networks, *Computers & Structures* 81 (28–29) (2003) 2631–2644.
[22] J.L. Wojtowicki, L. Jaouen, New approach for the measurements of damping properties of materials using oberst beam, *Review of Scientific Instruments* 75 (8) (2004) 2569–2574.
[23] K. Vanhoenacker, J. Schoukens, P. Guillaume, S. Vanlanduit, The use of multisine excitations to characterise damage in structures, *Mechanical Systems and Signal Processing* 18 (2004) 43–57.
[24] R.M. Gadelrab, The effect of delamination on the natural frequencies of a laminated composite beam, *Journal of Sound and Vibration* 197 (3) (1996) 283–292.
[25] J.J. Tracy, G.C. Pardoen, Effect of delamination on the natural frequencies of composite laminates, *Journal of Composite Materials* 23 (12) (1989) 1200–1215.
[26] A. Shahdin, J. Morlier, Y. Gourinat, Correlating low energy impact damage with changes in modal parameters: a preliminary study on composite beams, *Structural Health Monitoring* 8 (6) (2009) 523–536.
[27] O.S. Salawu, Detection of structural damage through changes in frequency: a review, *Engineering Structures* 19 (9) (1996) 718–723.
[28] H.Y. Kim, W. Hwang, Effect of debonding on natural frequencies and frequency response functions of honeycomb sandwich beams, *Composite Structures* 55 (2002) 51–62.
[29] W. Lestari, P. Qiao, Damage detection of fiber-reinforced polymer honeycomb sandwich beams, *Composite Structures* 67 (2005) 365–373.
[30] R.D. Adams, P. Cawley, The localisation of defects in structures from measurements of natural frequencies, *Journal of Strain Analysis* 14 (1979) 49–57.
[31] L.H. Yam, L. Cheng, Damage detection of composite structures using dynamic analysis, *Key Engineering Materials* 295–296 (2005) 33–39.
[32] J.Z. Arkaduiz, Non-linear vibration of a delaminated composite beam, *Key Engineering Materials* 293–294 (2005) 607–614.
[33] J.T. Kim, Y.S. Ryu, H.M. Cho, N. Stubbs, Damage identification in beam-type structures: frequency-based method vs. mode-shape based method, *Engineering Structures* 25 (1) (2003) 57–67.
[34] L.M. Khoo, P.R. Mantena, P. Jadhav, Structural damage assessment using vibration modal analysis, *Structural Health Monitoring* 3 (2) (2004) 177–194.
[35] S.G. Mattson, S.M. Pandit, Damage detection and localization based on outlying residuals, *Smart Materials and Structures* 15 (2006) 1801–1810.
[36] D. Montalvao, A.M. Ribeiro, J. Duarte-Silva, A method for the localization of damage in a CFRP plate using damping, *Mechanical Systems and Signal Processing* (2008), doi:10.1016/j.ymssp.2008.08.011.
[37] R.D. Adams, Damping in composites, *Material Science Forum* 119–121 (1993) 3–16.
[38] Z. Zhang, G. Hartwig, Relation of damping and fatigue damage of unidirectional fibre composites, *International Journal of Fatigue* 24 (2004) 713–738.
[39] R.F. Gibson, Modal vibration response measurements for characterization of composite materials and structures, *Composites Science and Technology* 60 (2000) 2769–2780.
[40] D.A. Saravanos, D.A. Hopkins, Effects of delaminations on the damped dynamic characteristics of composites, *Journal of Sound and Vibration* 192 (1995) 977–993.

[41] M. Colakoglu, Description of fatigue damage using a damping monitoring technique, *Turkish Journal of Engineering and Environmental Sciences* 27 (2003) 125–130.
[42] M.H. Richardson, M.A. Mannan, Correlating minute structural faults with changes in modal parameters, *Proceedings of SPIE, International Society for Optical Engineering* 1923 (2) (1993) 893–898.
[43] HexPly M21, Data Sheet, *Hexcel Composites*, F.R.
[44] HexWeb™, Honeycomb attributes and properties, *Hexcel Composites*, F.R.
[45] R.H. Meyers, D.C. Montgomery, *Response Surface Methodology*, Wiley, New York, 1995.
[46] J. Morlier, B. Chermain, Y. Gourinat. Original statistical approach for the reliability in modal parameters, *Proceedings of the International Modal Analysis Conference*, IMAC XXVII 2009.
[47] B. Peeters, H.V. Auweraer, P. Guillaume, J. Leuridan, The PolyMAX frequency–domain method: a new standard for modal parameter estimation, *Shock and Vibrations* 11 (2004) 395–409.